Journal of Statistical Physics, Vol. 17, No. 5, 1977

Statistical Mechanics of Two-Dimensional Vortices

T. S. Lundgren[1,2] and Y. B. Pointin[1]

Received April 26, 1977

Equilibrium statistics of a cluster of a large number of positive two-dimensional point vortices in an infinite region and the associated thermodynamic functions, exhibiting negative temperatures, are evaluated analytically and numerically from a microcanonical ensemble. Extensive numerical simulations of vortex motion are performed to verify the predicted equilibrium configurations. An application of Kubo's linear response theory is used to study the nonequilibrium situation that results from placing a cluster of vortices in a weak external velocity field, such as that produced by a distant vortex cluster. The weak field causes the cluster to grow in size as if there were an effective positive eddy viscosity. When a number of clusters interact, the effect is for each to grow while the distances between them decrease with time. The latter effect is an exhibit of negative viscosity. The application of this to the motion of the atmosphere is discussed.

KEY WORDS: Statistical mechanics; two-dimensional vortices; negative temperature; negative viscosity.

1. INTRODUCTION

In a number of papers,[1-5] as a numerical scheme, a two-dimensional incompressible vorticity field is discretized into vortices each of which is transported in the velocity field induced by all of the others. There is another class of problems studied where the discrete nature of the vortices is natural. These are the superfluid helium states, where discrete "quantized" vortices appear when the fluid is caused to rotate,[6-11] and in a two-dimensional magnetized plasma, where the motion of "two-dimensional" electrons and ions in a strong magnetic field is mathematically equivalent to vortex motion.[12-22]

Supported in part by National Science Foundation Grant GK-40263.

[1] Advanced Study Program, National Center for Atmospheric Research (sponsored by the National Science Foundation).

[2] Permanent address: Department of Aerospace Engineering and Mechanics, University of Minnesota, Minneapolis, Minnesota.

The present paper will be restricted to the statistical mechanics of the very simplest case of a large number of vortices of one kind in an infinite region. All previous papers of a statistical nature have considered finite regions. The restriction to an infinite region is made partly for numerical reasons; the equations are simpler without boundaries. The restriction to one species of vortex is related to this because vortices of opposite kinds will pair up and propagate out to infinity. There can be no equilibrium configuration with equal numbers of vortices of two kinds in an infinite region.

The best application would appear to be to the atmosphere, where cyclonic vorticity is more dominant than anticyclonic vorticity.[24] In a very loose model one can view the earth as a plane with the north pole at the center and the equator at infinity. The motion in this plane is induced by clusters of vortices, which represent cyclones. The effect of Coriolis forces could be included here without qualitative difference.

The paper is organized into three main parts. In the first part (Section 2) the equilibrium statistics are worked out giving the distribution of vortices in an isolated cluster and the associated thermodynamic functions. The average density of vortices is found to be axially symmetric, being more peaked at the center, and hence more highly ordered, for states of high energy. By the classical definition of entropy and temperature, this gives states with negative temperature, which are peculiar in no other way.

The second part (Section 3) involves direct numerical integration of the vortex equations of motion with the intention of verifying the equilibrium configurations. It is found that if the system is started in a configuration that is not too far from equilibrium, it will evolve in a relatively short time toward the equilibrium configuration. However, if the system is started far from equilibrium, as, for instance, when the starting state consists of two widely separated clusters, the system appears not to tend to equilibrium. The two clusters remain intact and continue to orbit each other for as long as computation is practical. The third part (Section 4) of the paper addresses this problem by studying the weak nonequilibrium situation that arises when a cluster of vortices is placed in a weak external velocity field, such as that produced by a distant cluster of vortices. By using linear response theory, it is concluded that two distant orbiting clusters will eventually coalesce.

The implications for the atmospheric model are that the interacting clusters, representing cyclones, will eventually coalesce into a single polar equilibrium cluster. In the process, angular momentum flows from the small-scale individual clusters into the larger equilibrium cluster. In the atmosphere this "inverse angular momentum cascade" compensates for frictional losses in the westerly winds.[25]

The equations of motion of a system of point vortices express that each vortex drifts in the incompressible velocity field produced at its position by

the superposition of the velocity fields of each of the other vortices. In an infinite region the velocity at the position of the ith vortex due to the jth, of strength Γ, is $\hat{\mathbf{z}} \times (\partial/\partial \mathbf{r}_i)[\Gamma(\ln r_{ij})/2\pi]$, perpendicular to the line of centers of the two vortices, with magnitude $\Gamma/2\pi r_{ij}$. The equations may be written in the form shown by Kirchhoff,[26]

$$\Gamma \frac{d\mathbf{r}_i}{dt} = -\hat{\mathbf{z}} \times \frac{\partial}{\partial \mathbf{r}_i} \mathscr{H}(\mathbf{r}_1, \mathbf{r}_2, \ldots, \mathbf{r}_N), \qquad i = 1, 2, \ldots, N \tag{1}$$

where

$$\mathscr{H} = -\sum_{i,j,i>j} \frac{\Gamma^2 \ln r_{ij}/l_0}{2\pi}, \qquad r_{ij} = |\mathbf{r}_i - \mathbf{r}_j| \tag{2}$$

The parameter l_0 is an arbitrary length, carried along to keep the argument of the logarithm dimensionless. It is easily shown[26] that the Hamiltonian $\mathscr{H}$ is a constant of the motion, as are $\sum_{i=1}^{N} r_i^2$ and $\sum_{i=1}^{N} \mathbf{r}_i$.

The quantity $\rho\mathscr{H}$, where ρ is the mass of the fluid per unit area, is called the interaction energy and is the kinetic energy of the fluid minus the "infinite" self-energy of the vortices. In a similar manner, $-\frac{1}{2}\rho\Gamma \sum_{i=1}^{N} r_i^2$ is related to the angular momentum of the fluid.

The third constant shows that the center of vorticity

$$\mathbf{R} = \frac{1}{N} \sum_{i=1}^{N} \mathbf{r}_i \tag{3}$$

stays fixed. A constant length L, related to the angular momentum relative to the center of vorticity, may be defined by

$$L^2 = \frac{1}{N} \sum_{i=1}^{N} (\mathbf{r}_i - \mathbf{R})^2 \tag{4}$$

This constant of motion prevents vortices from diffusing far from the center of vorticity.

2. EQUILIBRIUM STATISTICAL MECHANICS

Let $P_N(\mathbf{r}_1, \mathbf{r}_2, \ldots, \mathbf{r}_N; t)$ denote the probability density for the system of vortices, defined such that $P_N\, d\mathbf{r}_1\, d\mathbf{r}_2 \cdots d\mathbf{r}_N$ is the probability that $\mathbf{r}_1$ is in $d\mathbf{r}_1$, $\mathbf{r}_2$ in $d\mathbf{r}_2$, etc. A Liouville equation,[27] expressing conservation of probability, may be written

$$\frac{\partial P_N}{\partial t} + \sum_{i=1}^{N} \frac{1}{\Gamma} \left(-\hat{\mathbf{z}} \times \frac{\partial \mathscr{H}}{\partial \mathbf{r}_i} \right) \cdot \frac{\partial P_N}{\partial \mathbf{r}_i} = 0 \tag{5}$$

It is clear that any function of the constants of motion of Eq. (1) is a time-independent solution, Eq. (5). It is a basic hypothesis of statistical mechanics

that, in an equilibrium situation, P_N is a function of the single-valued integrals of motion, the isolating integrals,[28] which are presumably only those already mentioned.

Of the several classical forms taken for this function, the microcanonical ensemble

$$P_N = \delta(\rho\mathscr{H} - E)\,\delta\left(\sum_{i=1}^{N}(\mathbf{r}_i - \mathbf{R})^2 - NL^2\right)\delta\left(\sum_{i=1}^{N}\mathbf{r}_i - N\mathbf{R}\right)\Big/ Q(E, L^2) \quad (6)$$

is appropriate here since it represents an ensemble of isolated systems with nonfluctuating constants E, L^2, $\mathbf{R}$. This formula expresses the assumption that equal areas of the intersection of the hypersurfaces, described by the delta functions, are equally likely. It is further assumed, in order for the formula to make physical sense, that time averages over states seen by one member of the ensemble are the same as ensemble averages (ergodic hypothesis).[28] A sufficient, but not necessary, condition for this to be true is that an actual system spend equal times in equal areas of this hypersurface.[29]

Since $\int P_N\, d\mathbf{r}_1 \cdots d\mathbf{r}_N = 1$, the normalizing factor Q must satisfy

$$Q(E, L^2) = \int \delta(\rho\mathscr{H} - E)\,\delta\left(\sum_{i=1}^{N}(\mathbf{r}_i - \mathbf{R})^2 - NL^2\right)\delta\left(\sum_{i=1}^{N}\mathbf{r}_i - N\mathbf{R}\right) d\mathbf{r}_1 \cdots d\mathbf{r}_N \quad (7)$$

It is clear that Q does not depend on $\mathbf{R}$, since $\mathbf{R}$ may be absorbed by a shift of origin in the integral. The function Q is called the "density of states," since it is proportional to the area cut out of phase space by the isolating integrals.

In classical thermodynamics,[30,31] the entropy of the system is defined by

$$S(E, L^2) = k \ln Q \quad (8)$$

and the temperature by

$$1/T = \partial S(E, L^2)/\partial E \quad (9)$$

or

$$1/kT = (1/Q)\,\partial Q/\partial E$$

It was first pointed out by Onsager,[12] for a vortex system similar to this, that the entropy as a function of E has a maximum value at some critical value of E and that states with E greater than this value possess negative temperatures,[15] because they are more ordered states. As E approaches E_{cr} from the left, $T \to +\infty$ and jumps to $-\infty$ as E_{cr} is passed. Onsager's argument is for a finite phase space; the existence of the additional constant of the motion L^2 plays that role here.

A hierarchy of reduced probability densities may be defined by

$$P_1(\mathbf{r}_1) = \int P_N \, d\mathbf{r}_2 \cdots d\mathbf{r}_N, \qquad P_2(\mathbf{r}_1, \mathbf{r}_2) = \int P_N \, d\mathbf{r}_3 \cdots d\mathbf{r}_N$$

and so on. These reduced densities are related to more physical quantities. Let

$$n(\mathbf{r}) = \sum_{i=1}^{N} \delta(\mathbf{r} - \mathbf{r}_i) \tag{10}$$

be the actual number density of vortices. Then

$$\langle n(\mathbf{r}) \rangle = \sum_{i=1}^{N} \langle \delta(\mathbf{r} - \mathbf{r}_i) \rangle = N P_1(\mathbf{r}) \tag{11}$$

relates P_1 to the average density of vortices.

The vorticity in this system of vortices is given by

$$\omega(\mathbf{r}) = \Gamma n(\mathbf{r}) = \sum_{i=1}^{N} \Gamma \, \delta(\mathbf{r} - \mathbf{r}_i) \tag{12}$$

and the velocity may be determined from the stream function ψ by

$$\mathbf{v} = -\hat{\mathbf{z}} \times \nabla \psi$$

where

$$\psi = -\int \frac{\ln|\mathbf{r} - \mathbf{r}'|}{2\pi} \, \omega(\mathbf{r}') \, d\mathbf{r}'$$

Therefore the average vorticity and average velocity

$$\langle \omega(\mathbf{r}) \rangle = N\Gamma P_1(\mathbf{r}) \tag{13}$$

$$\langle \mathbf{v}(\mathbf{r}) \rangle = \frac{N\Gamma}{2\pi} \int \left(\hat{\mathbf{z}} \times \frac{\partial}{\partial \mathbf{r}} \ln |\mathbf{r} - \mathbf{r}'| \right) P_1(\mathbf{r}') \, d\mathbf{r}' \tag{14}$$

are related to the one-point distribution.

The average value of the energy and "angular momentum" are given in terms of P_2 and P_1 by

$$E = \langle \rho \mathscr{H} \rangle = -\frac{1}{2}(N^2 - N) \frac{\rho \Gamma^2}{2\pi} \int \ln \frac{r_{12}}{l_0} P_2(\mathbf{r}_1, \mathbf{r}_2) \, d\mathbf{r}_1 \, d\mathbf{r}_2 \tag{15}$$

and

$$NL^2 = \left\langle \sum_{i=1}^{N} (\mathbf{r}_i - \mathbf{R})^2 \right\rangle = N \int (\mathbf{r}_1 - \mathbf{R})^2 P_1(\mathbf{r}_1) \, d\mathbf{r}_1 \tag{16}$$

Note that in Eq. (15), $P_2(\mathbf{r}_1, \mathbf{r}_2)$ may be decomposed as $P_1(\mathbf{r}_1)P_1(\mathbf{r}_2) + P_2'(\mathbf{r}_1, \mathbf{r}_2)$. The first term contributes the part of the interaction energy

associated with the mean flow. The second term, then, is the part associated with fluctuations from the mean flow.

Instead of obtaining the thermodynamic functions by evaluating Q from Eq. (7) directly, this will be done by calculating the reduced distribution functions, in a self-consistent way, and then calculating the energy from Eq. (15).

2.1. Hierarchy of Equations for the Reduced Distribution Functions

Using Eq. (6), P_1 is defined by

$$P_1(\mathbf{r}_1) = Q(E, L^2)^{-1} \times \int \delta(\rho\mathscr{H} - E)\, \delta\Big(\sum (\mathbf{r}_i - \mathbf{R})^2 - NL^2\Big)\, \delta\Big(\sum \mathbf{r}_i - N\mathbf{R}\Big)\, d\mathbf{r}_2 \cdots d\mathbf{r}_N \tag{17}$$

Differentiating this function with respect to $\mathbf{r}_1$, which occurs in the arguments of the delta functions in $\mathscr{H}$, $\sum (\mathbf{r}_i - \mathbf{R})^2$, and $\sum \mathbf{r}_i$, we obtain

$$\frac{\partial P_1(\mathbf{r}_1)}{\partial \mathbf{r}_1} = \frac{(N-1)\rho\Gamma^2}{2\pi} \int \frac{\partial \ln r_{21}}{\partial \mathbf{r}_1} \frac{1}{Q} \frac{\partial}{\partial E} QP_2(\mathbf{r}_1, \mathbf{r}_2)\, d\mathbf{r}_2 - 2(\mathbf{r}_1 - \mathbf{R}) \frac{1}{Q} \frac{\partial}{\partial NL^2} QP_1(\mathbf{r}_1) - \frac{1}{Q} \frac{\partial}{\partial N\mathbf{R}} QP_1(\mathbf{r}_1) \tag{18}$$

The procedure leading to Eq. (18) may be repeated for the two-point distribution, the three-point distribution, and so on.

By differentiating the defining relation for $P_S(\mathbf{r}_1, \ldots, \mathbf{r}_S)$, the general result may be obtained,

$$\frac{\partial P_S(\mathbf{r}_1, \ldots, \mathbf{r}_S)}{\partial \mathbf{r}_1} = \left[\frac{\rho\Gamma^2}{2\pi} \left(\sum_{j=2}^{S} \frac{\partial \ln r_{j1}}{\partial \mathbf{r}_1}\right) \frac{1}{Q} \frac{\partial}{\partial E} QP_S + \frac{(N-S)\rho\Gamma^2}{2\pi} \int \left(\frac{\partial}{\partial \mathbf{r}_1} \ln r_{S+1,1}\right) \frac{1}{Q} \frac{\partial}{\partial E} QP_{S+1}(\mathbf{r}_1, \ldots, \mathbf{r}_{S+1})\, d\mathbf{r}_{S+1}\right] - 2(\mathbf{r}_1 - \mathbf{R}) \frac{1}{Q} \frac{\partial}{\partial NL^2} QP_S - \frac{1}{Q} \frac{\partial}{\partial N\mathbf{R}} QP_S \tag{19}$$

Each equation in the hierarchy introduces a distribution function one step higher in order into the basic relationship, so that at any level there is always one more unknown than the number of equations available.

It will be noted that in these equations there are awkward terms like $(1/Q)\,\partial QP_s/\partial E$. By using Eq. (9) this may be written

$$\frac{1}{Q}\frac{\partial}{\partial E}QP_s = \frac{1}{kT}P_s + \frac{\partial P_s}{\partial E} \tag{20}$$

The second term on the right is difficult. It would not have occurred if the derivation had started from the exponential form canonical ensemble instead of Eq. (18). It will be shown later that, in fact, the second term is negligible compared to the first.

A formula similar to Eq. (20) may be devised for $(1/Q)\,\partial QP_s/\partial NL^2$, namely

$$\frac{1}{Q}\frac{\partial}{\partial NL^2}QP_s = \frac{1}{Q}\frac{\partial Q}{\partial NL^2}P_s + \frac{\partial P_s}{\partial NL^2} \tag{21}$$

where

$$\frac{1}{Q}\frac{\partial Q}{\partial NL^2} = \frac{1}{L^2}\left(1 + \frac{\partial N\Gamma^2}{8\pi kT}\right) \tag{22}$$

To establish Eq. (22), a procedure similar to the equation of state derivation of Salzberg and Prager[32] is used. In Eq. (7), defining Q, the change of the variable of integration to $\boldsymbol{\rho}_i = (\mathbf{r}_i - \mathbf{R})/L$ gives

$$Q = L^{2(N-1)}\int \delta\left(-\sum_{i,j,i>j}\frac{\rho\Gamma^2}{2\pi}\ln\rho_{ij} - E'\right)\delta\left(\sum\rho_i{}^2 - N\right)\delta\left(\sum\rho_i\right)d\boldsymbol{\rho}_1\cdots d\boldsymbol{\rho}_N \tag{23}$$

where

$$E' = E + \frac{\rho\Gamma^2}{2\pi}\frac{N^2 - N}{2}\ln\frac{L}{l_0} \tag{24}$$

There is no additional dependence on L since the region of integration is infinite. From this it is clear that

$$\frac{\partial \ln Q}{\partial E} = \frac{\partial \ln Q}{\partial E'} = \frac{1}{kT} \tag{25}$$

and

$$\frac{\partial \ln Q}{\partial L^2} = \frac{N-1}{L^2} + \frac{\rho\Gamma^2}{2\pi}\frac{N^2 - N}{4L^2}\frac{\partial \ln Q}{\partial E'} \tag{26}$$

from which Eq. (22) follows. A similar formula for $(1/Q)\,\partial QP_s/\partial\mathbf{R}$ is unnecessary since Q is independent of $\mathbf{R}$.

Note that by using Eqs. (22) and (25) a form of Gibbs equation may be written:

$$\begin{aligned} dS &= \frac{\partial S}{\partial E}dE + \frac{\partial S}{\partial L^2}dL^2 \\ &= \frac{1}{T}dE + kN\left(1 + \frac{\rho N\Gamma^2}{8\pi kT}\right)\frac{dL^2}{L^2} \end{aligned} \tag{27}$$

2.2. Closure of the One-Point Equation

It is proposed that Eq. (18) be closed by replacing $P_2(\mathbf{r}_1, \mathbf{r}_2)$ by $P_1(\mathbf{r}_1)P_1(\mathbf{r}_2)$. This is a common closure in kinetic theory, especially for plasmas. It has been used by Montgomery and Joyce[21] in a context similar to this. This approximation may be justified by showing that the higher order multipoint cumulant distribution functions P_s', which satisfy equations derived from Eq. (19), may be expanded, in a self-consistent manner, in the form $P_s' = O(\lambda/N)^{s-1}$, where

$$\lambda = \rho N \Gamma^2 / 8\pi kT \tag{28}$$

Thus

$$P_2(\mathbf{r}_1, \mathbf{r}_2) - P_1(\mathbf{r}_1)P_1(\mathbf{r}_2) \equiv P_2'(\mathbf{r}_1, \mathbf{r}_2) = O(\lambda/N) \tag{29}$$

is small if λ/N is small. The parameter λ/N may be identified as the two-dimensional version of the "plasma parameter."[33]

It may also be shown that the second terms in Eqs. (20) and (21) are negligible if N is sufficiently large, as is also the case for $(1/N)\,\partial P_1/\partial \mathbf{R}$. The resulting equation is

$$\frac{\partial P_1(\mathbf{r}_1)}{\partial \mathbf{r}_1} = 4\lambda \int \left(\frac{\partial}{\partial \mathbf{r}_1} \ln r_{21}\right) P_1(\mathbf{r}_2)P_1(\mathbf{r}_1)\, d\mathbf{r}_2 - 2(\mathbf{r}_1 - \mathbf{R}) \frac{1 + \lambda}{L^2} P_1(\mathbf{r}_1) \tag{30}$$

This is to be solved with the normalizing condition $\int P_1(\mathbf{r}_1)\, d\mathbf{r}_1 = 1$. The condition given by Eq. (16), which defines L, will then be satisfied automatically.

With the change of variables

$$\tilde{P}_1(\boldsymbol{\eta}) = L^2 P_1(\mathbf{r}_1), \qquad \boldsymbol{\eta} = (\mathbf{r}_1 - \mathbf{R})/L \tag{31}$$

Eq. (30) may be written

$$\frac{\partial}{\partial \boldsymbol{\eta}_1} \ln \tilde{P}_1 = 4\lambda \int \left(\frac{\partial}{\partial \boldsymbol{\eta}_1} \ln \eta_{21}\right) \tilde{P}_1(\boldsymbol{\eta}_2)\, d\boldsymbol{\eta}_2 - 2(1 + \lambda)\boldsymbol{\eta}_1 \tag{32}$$

The procedure is to solve this for $\tilde{P}_1$ for each value of the parameter λ, which is a dimensionless inverse temperature, and to use this to compute the energy from Eq. (15), which, with the product form for P_2, may be written

$$E = \rho N^2 \Gamma^2 [\tilde{E}(\lambda) - (1/4\pi) \ln(L/l_0)]$$

where

$$\tilde{E}(\lambda) = -\frac{1}{4\pi} \int \ln \eta_{12}\, \tilde{P}_1(\boldsymbol{\eta}_1)\tilde{P}_1(\boldsymbol{\eta}_2)\, d\boldsymbol{\eta}_1\, d\boldsymbol{\eta}_2 \tag{33}$$

is a function of λ alone, thus obtaining the thermodynamic functions. To this end, Eq. (32) may be integrated once, casting it in the form of an integral equation

$$\tilde{P}_1(\boldsymbol{\eta}_1) = C_1 \exp\left[-(1 + \lambda)\eta_1^2 + 4\lambda \int \ln \eta_{21} \tilde{P}_1(\boldsymbol{\eta}_2)\, d\boldsymbol{\eta}_2\right] \tag{34}$$

The constant of integration C_1 is to be determined from the condition $\int \tilde{P}_1(\boldsymbol{\eta}_1)\, d\boldsymbol{\eta}_1 = 1$.

Several results follow directly from Eq. (34). If $\lambda = 0$, the solution is Gaussian,

$$\tilde{P}_1(\boldsymbol{\eta}_1) = (1/\pi) \exp(-\eta_1^2) \tag{35}$$

For very large η_1, the asymptotic behavior of $\tilde{P}_1$ is

$$\tilde{P}_1 \sim C_1 \{\exp[-(1 + \lambda)\eta_1^2]\} \eta_1^{4\lambda} \tag{36}$$

from which one sees that $\lambda \geqslant -1$ is required for the existence of an integrable solution.

An alternate approach is to take the divergence of Eq. (32) using $\nabla^2 \ln \eta = 2\pi\delta(\boldsymbol{\eta})$. This gives

$$\frac{\partial}{\partial \boldsymbol{\eta}_1} \cdot \frac{\partial}{\partial \boldsymbol{\eta}_1} \ln \tilde{P}_1 = 8\pi\lambda \tilde{P}_1 - 4(1 + \lambda) \tag{37}$$

or, since $\tilde{P}_1$ must depend only on the magnitude of $\boldsymbol{\eta}_1$, the ordinary nonlinear differential equation

$$\frac{d^2 \ln \tilde{P}_1}{d\eta^2} + \frac{1}{\eta} \frac{d \ln \tilde{P}_1}{d\eta} = -4(1 + \lambda) + 8\pi\lambda \exp(\ln \tilde{P}_1) \tag{38}$$

The results of the numerical integration of this equation are shown in Fig. 1 for selected values of λ. For positive λ, which corresponds to positive temperature, the vortex density $\tilde{P}_1$ is relatively flat near the center. For negative λ the vortex density is more peaked in the center, getting sharper as $\lambda \to -1$.

Certain asymptotic results can be obtained analytically. In the limit as $\lambda \to \infty$ it is easily seen from Eq. (38) that the solution is

$$\begin{aligned} \tilde{P}_1 &= 1/2\pi, \qquad \eta < \sqrt{2} \\ &= 0 \qquad\quad \eta > \sqrt{2} \end{aligned} \tag{39}$$

As $\lambda \to -1$, an approximate solution is

$$\tilde{P}_1 = \frac{A}{(1 - \pi\lambda A \eta^2)^2} \exp[-(1 + \lambda)\eta^2] \tag{40}$$

The first factor is an exact solution of Eq. (38) with the first term on the right-hand side neglected. The second factor is a correction for large η, in agreement with the asymptotic result expressed by Eq. (36). The parameter

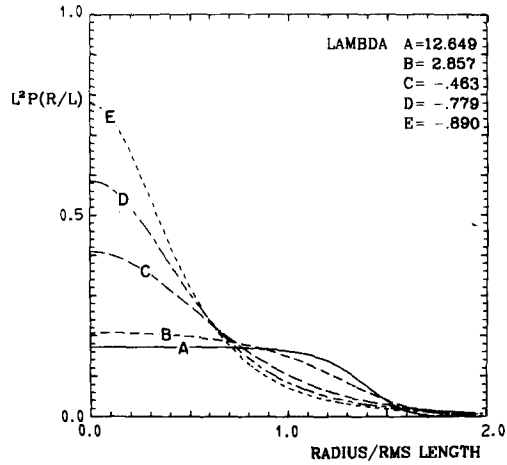

Fig. 1. Equilibrium vortex density vs. radial coordinate. The more peaked distributions correspond to higher energy levels.

A tends to infinity as $\lambda \to -1$ and is determined from the condition $\int \tilde{P}_1 \, d\tau = 1$ by the formula

$$\pi A + \ln \pi A = -\gamma - \ln(1 + \lambda), \qquad \gamma = 0.557 \tag{41}$$

which says, essentially, that A grows slowly as $\lambda \to -1$.

2.3. The Thermodynamic Functions

The relationship between energy and temperature may be obtained by substituting the numerical solution for $\tilde{P}_1$ (for each λ) into Eq. (33) after first carrying out the integrations on the angle variables. The results of this calculation are shown in Fig. 2. It should be noted that the range of negative temperatures is such that $\lambda > -1$.

Having obtained the relationship between energy and temperature, we can determine the entropy from Eq. (27), using Eq. (33), in the form

$$S/kN = \int^{\tilde{E}} 8\pi\lambda(\tilde{E}) \, d\tilde{E} + \ln L^2 \tag{42}$$

However, it may be shown that the classical definition of entropy,[30]

$$S/kN = \tilde{S}(\lambda) + \ln L^2 + \text{const} \tag{43}$$

$$\tilde{S} = -\int \tilde{P}_1(\eta) \ln \tilde{P}_1(\eta) \, 2\pi\eta \, d\eta \tag{44}$$

is equivalent to Eq. (42) and the latter quantity can be more easily computed. The results of this calculation are shown in Fig. 3.

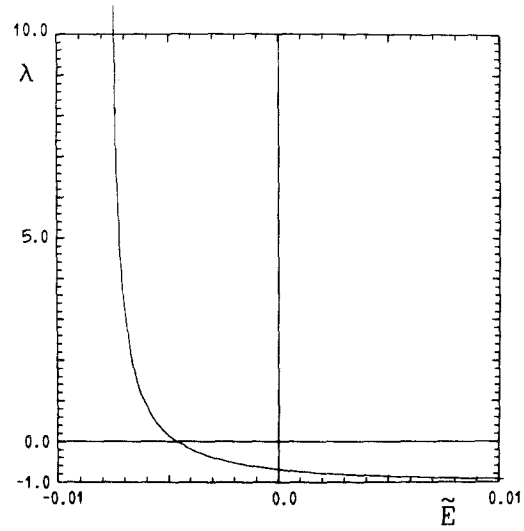

Fig. 2. Dimensionless reciprocal temperature λ vs. energy.

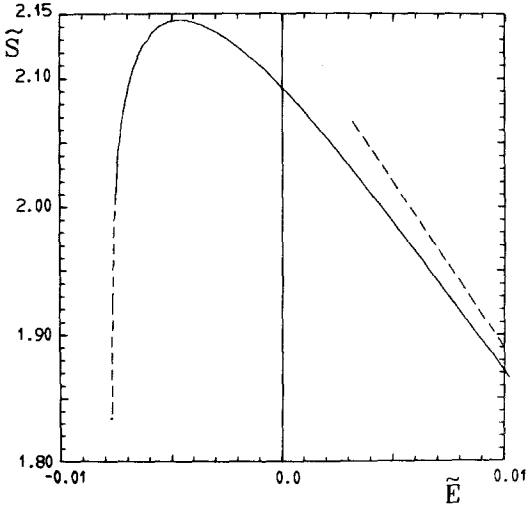

Fig. 3. Dimensionless entropy vs. energy. Maximum entropy occurs at an energy where λ in Fig. 2 is zero.

It should be noted here that Eq. (34) can also be derived from a variational principle by maximizing the entropy, defined by Eq. (44), subject to the constraints that the energy (in the product form), $\int r^2 P_1(\mathbf{r})\, d\mathbf{r}$ and $\int P_1(\mathbf{r})\, d\mathbf{r}$ be fixed. This was the method used by Joyce and Montgomery[18] for a similar problem in a rectangular domain. It is felt that the present method is slightly superior since the variational derivation has undetermined Lagrange multipliers, which have to be identified in terms of T and L^2 by some other argument. More importantly, the closure method allows the error involved to be examined by investigating higher order distribution functions.

There are analytical landmarks that can be identified in Figs. 2 and 3. When $\lambda = 0$, P_1 is given by Eq. (35) and $E(\lambda)$ and $S(\lambda)$ can be computed, giving

$$\begin{aligned} \tilde{E}(0) &= (1/8\pi)(\gamma - \ln 2) = -0.00461, \qquad \gamma = 0.577 \\ \tilde{S}(0) &= 1 + \ln \pi = 2.1447 \end{aligned} \tag{45}$$

The former number is the value of the energy where the temperature changes signs, the latter the maximum value of the entropy.

Similarly, as $\lambda \to \infty$ the solution is given by Eq. (39) and

$$\begin{aligned} \tilde{E}(\lambda = \infty) &= -(1/16\pi)(2 \ln 2 - 1) = -0.00769 \\ \tilde{S}(\lambda = \infty) &= \ln 2\pi = 1.8379 \end{aligned} \tag{46}$$

This energy is the lowest value that occurs and $\tilde{S}$ is the corresponding entropy.

As $\lambda \to -1$ the solution is given by Eq. (40). By substituting this into the integrals for $\tilde{E}$ and $\tilde{S}$ and using Eq. (41), the following asymptotic formulas can be derived:

$$\begin{aligned} \lambda &= -1 + \exp[-1.5772 - 8\pi\tilde{E} - \exp(1 + 8\pi\tilde{E})] \\ \tilde{S} &= 1 + \ln \pi - 8\pi\tilde{E} \end{aligned} \tag{47}$$

The latter result is shown as a straight line on Fig. 3. The former shows how $-\lambda$ tends to unity as $\tilde{E} \to \infty$. It is apparently valid only for larger values of $\tilde{E}$ than those on Fig. 2 since the decay to minus one is extremely rapid. This tendency for the temperature to approach a constant, negative value as energy tends to infinity is also a feature of the work of other authors.[19,20]

3. NUMERICAL SIMULATION OF VORTEX MOTION

In Section 2 considerable space is devoted to developing approximations to the theoretical equilibrium distribution of vortex clusters. The purpose of

the present section and the next is twofold, to verify the theoretical distribution by numerical simulations and to show that starting from some other distribution of vortices, the system will tend to the equilibrium distribution with time. The latter is the more difficult since the approach to equilibrium is slow in some cases.

Equation (1) may be written in a form more convenient for numerical purposes as

$$\begin{aligned} \frac{dx_i}{dt} &= -\frac{2\pi}{N} \sum_{j=1, j\neq i}^{N} \frac{y_i - y_j}{(x_i + x_j)^2 + (y_i - y_j)^2} \\ \frac{dy_i}{dt} &= \frac{2\pi}{N} \sum_{j=1, j\neq i}^{N} \frac{x_i - x_j}{(x_i - x_j)^2 + (y_i - y_j)^2} \end{aligned} \tag{48}$$

$2N$ equations for the N vortex coordinate pairs (x_i, y_i). In these equations all coordinates have been made dimensionless by scaling with the length L. The time variable in Eq. (48) is made dimensionless with the characteristic turnaround time

$$T = (2\pi L)^2/N\Gamma \tag{49}$$

which would be the circulation time for a fluid particle at distance L from the origin if all the vorticity were concentrated there.

The initial-value problem for these equations has been solved by an eighth-order predictor-corrector method with a variable time increment, which ensures that the maximum error between the predicted and the corrected values lies between fixed bounds, usually 10^{-8}–10^{-10}. The method used is a modification of one developed by Nordsieck.[34]

The equations are integrated for various initial conditions in which the values of the constants of motion are either specified or computed. The initial values

$$\frac{1}{N} \sum_{i=1}^{N} x_i = 0 \tag{50}$$

$$\frac{1}{N} \sum_{i=1}^{N} y_i = 0 \tag{51}$$

$$\frac{1}{N} \sum_{i=1}^{N} (x_i^2 + y_i^2) = 1 \tag{52}$$

are always imposed. The dimensionless Hamiltonian

$$\tilde{E} = -\frac{1}{2\pi N^2} \sum_{i,j,i>j} \ln[(x_i - x_j)^2 + (y_i - y_j)^2]^{1/2} \tag{53}$$

corresponds to the function $\tilde{E}$ defined by Eq. (33) and is the parameter needed to compare with the theoretical equilibrium solutions. The error control is such that these four integrals of the motion retain their initial values rigorously to about seven significant figures for typical runs.

The constancy of the integrals of motion is a necessary condition for accuracy but the only real measure is reversibility of the computation. That is, after a certain length of computation, one integrates backward in time to the initial time and compares the vortex positions with their initial positions. A modification of this procedure that shows both the nature of error growth and the reversibility of the computation is shown in Fig. 4. The computation is for 60 vortices with an energy level such that $\lambda \simeq 14$ if it were an equilibrium state. (The energy level will often be given in terms of λ. To get the energy use Fig. 2.) Two simultaneous computations are carried out. The second differs from the first only in the initial position of one vortex, which has been displaced by 0.001 unit. The upper curve in the figure is the root mean square error divided by its initial value, 0.001. The lower curve is the corresponding maximum individual error in position over all of the vortices. The error grows exponentially at a remarkable rate, having grown by a factor of 1000 in two time units (the turnaround time of a typical vortex is between one and two units). At this time both computations are reversed. The error in the reversed computation is shown by the dashed lines in the figure, which coincide with the solid lines until the computation is almost back to the initial time, when they begin to grow rapidly. The maximum error between

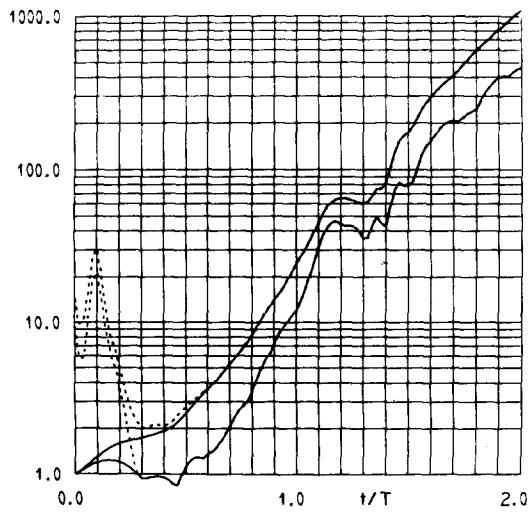

Fig. 4. Error growth analysis.

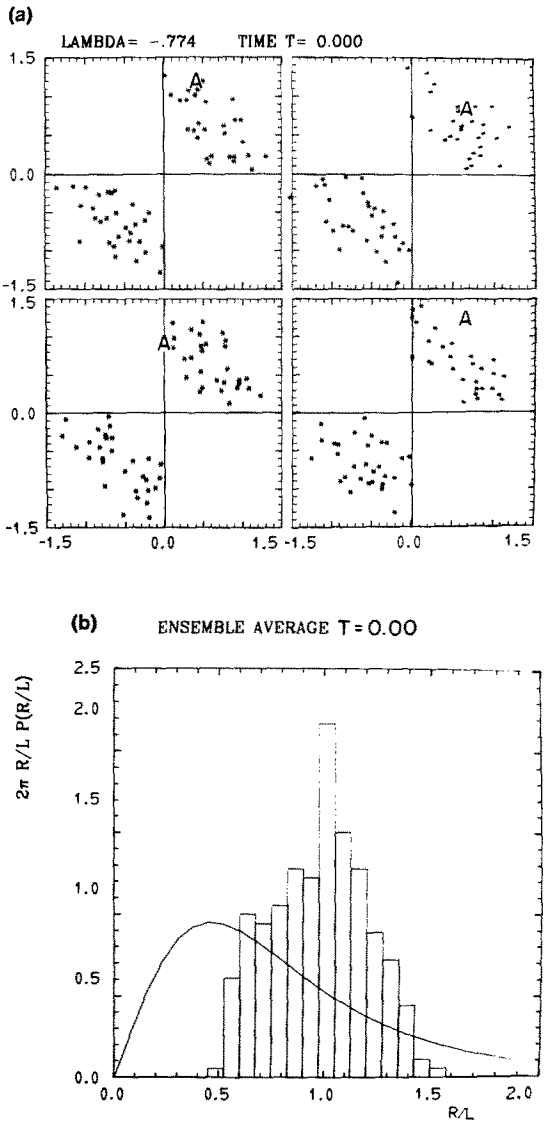

Fig. 5. Ensemble of four independent sets of 60 positive vortices in an infinite space with energy level specified by $\lambda = -0.774$. (a) The stars in each quadrant are the initial positions of the vortices in each of the four sets. The position of one vortex in each set is represented by the letter A. (b) A histogram of the ensemble average number of vortices in annular bands at the initial time compared with the predicted equilibrium vortex density (times radial coordinate). (c, d) Three turnaround time units after the start. (e, f) A total of 7.5 turnaround time units after the start. (g) Histogram of vortex positions for each member of the ensemble at 7.5 time units. (h) Ensemble- and time-averaged histogram from 6 to 7.5 time units.

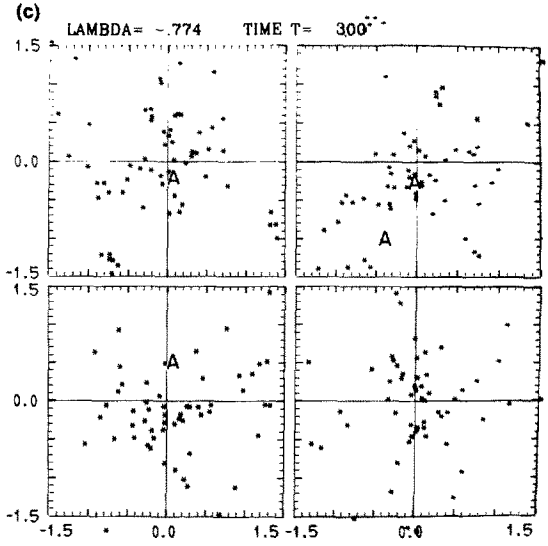

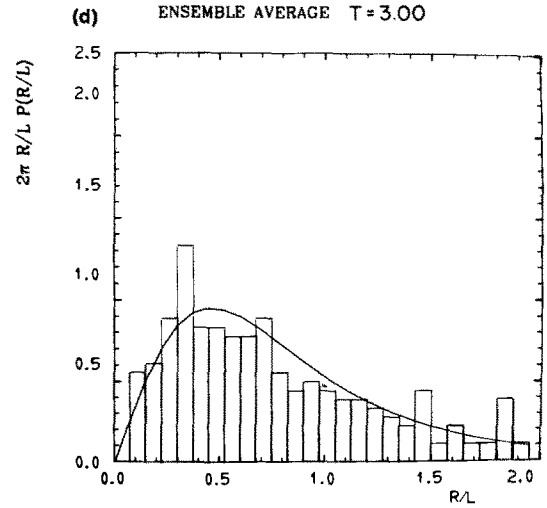

Fig. 5. Continued.

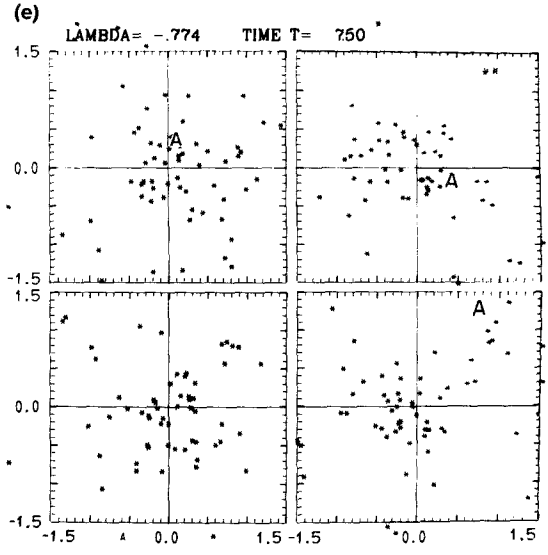

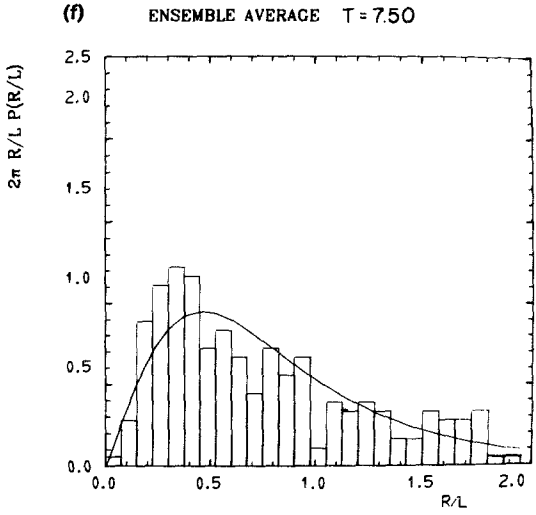

Fig. 5. Continued.

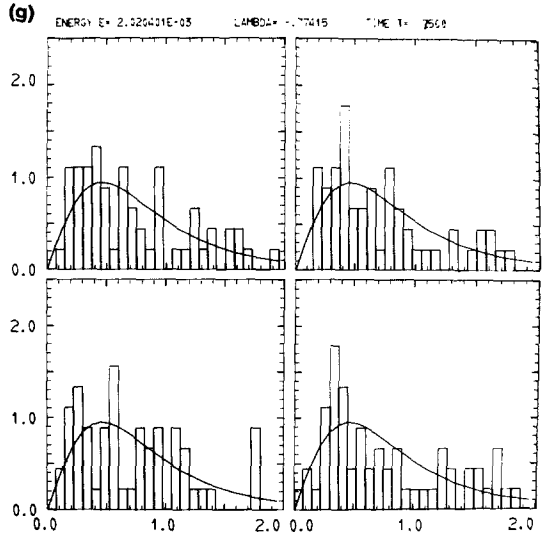

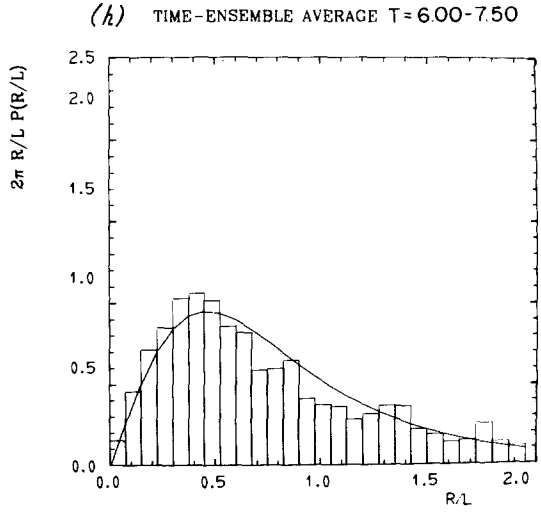

Fig. 5. Continued.

the positions of the vortices after this cycle and their initial positions is less than 0.01. Therefore errors have been controlled in the computations to the extent that they are almost error-free for four time units. Similar computations for higher energy levels are usually a little worse than this because the vortices have to be started closer together to get the larger energy.

A number of computations have been made with between 30 and 100 vortices. The fluctuations were quite large even with 100 vortices, which was already time-consuming. It was found to be economical to do computations with 60 vortices, repeating the computations for four sets of initial conditions and then ensemble-averaging the results. Such a computation takes about 15 min on NCAR's Control Data 7600.

Results are shown in Fig. 5, for an energy level corresponding to $\lambda = -0.774$. The vortices (stars on these figures) were separated into two clusters initially. Each cluster was restricted to lie between two radii, $\eta = 0.55$ and $\eta = 1.25$. They were picked randomly in these annuli, and then squeezed between two rays to get the desired energy level. In the figure the configuration of each of the four sets is shown for three times. At each time a figure with $2\pi\eta\tilde{P}_1(\eta)$ calculated from the equilibrium distribution is shown. On this figure a histogram of the average (over the four sets) number of vortices in each of 25 annular rings between $\eta = 0$ and $\eta = 2$ divided by the width of the ring is shown. At the last time shown, four histograms indicate the fluctuations in the various members of the ensemble. Also, a histogram involving both ensemble-averaging and time-averaging over the previous 1.5 time units is performed in order to smooth out these fluctuations. The tendency toward the equilibrium distribution is evident. Similar results for other energy levels could also be shown.

Two additional cases are shown in Figs. 6 and 7, which are at the same energy level as Fig. 5 but with three and four clusters, respectively. The three-cluster case appears to equilibrate; however, the four-cluster case appears not to do so. The computation in this case has been continued again as long without any apparent tendency to coalesce into a single vortex cluster.

4. EQUILIBRATION OF DISTANT CLUSTERS

In the last section the case of four tightly distributed clusters of vortices was found not to equilibrate during the relatively short time of the numerical integration. Similar situations have been found with two clusters and one would expect the same result with seven or fewer tight clusters of the same strength with centers equally spaced along a circle, since this is a configuration that has been found to be stable for point vortices.[35–37] Reasoning will be given to support the ultimate equilibration of such configurations.

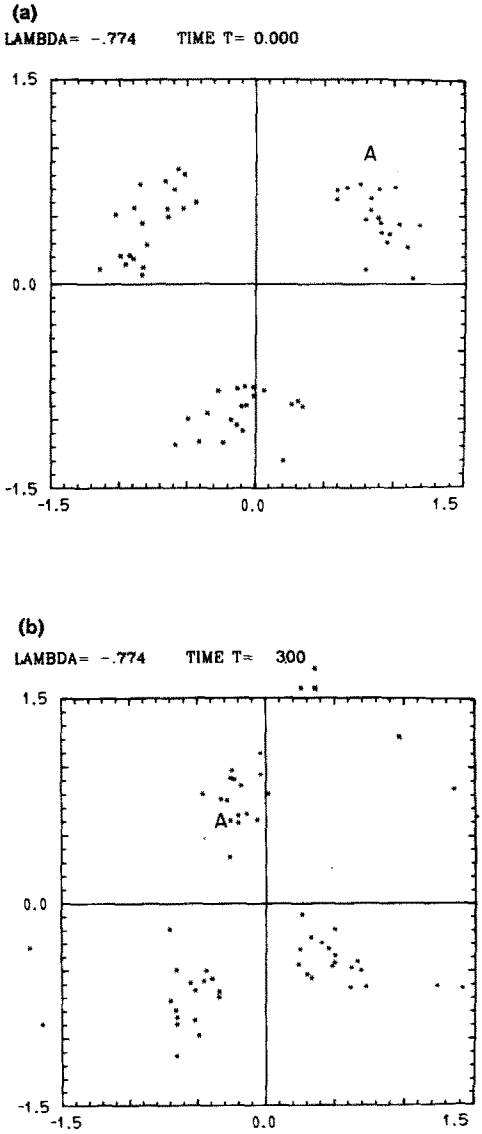

Fig. 6. Single set of 60 vortices in three-cluster initial configuration with energy level specified by $\lambda = -0.774$ as in Fig. (5), at (a) 0, (b) 3, and (c) 7.5 time units. (d) A time-averaged histogram from 6 to 7.5 time units.

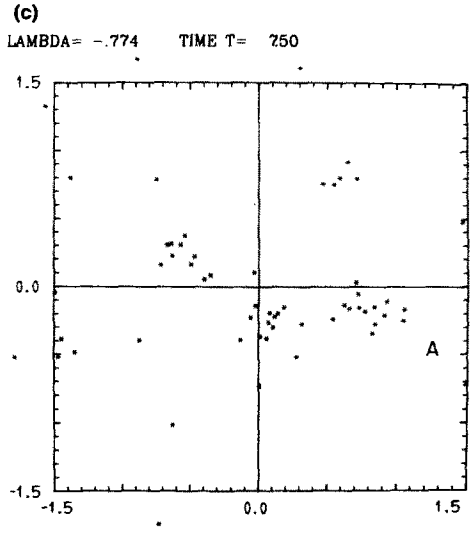

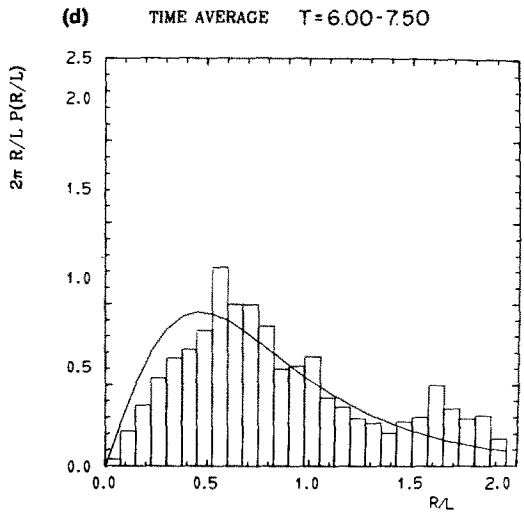

Fig. 6. Continued.

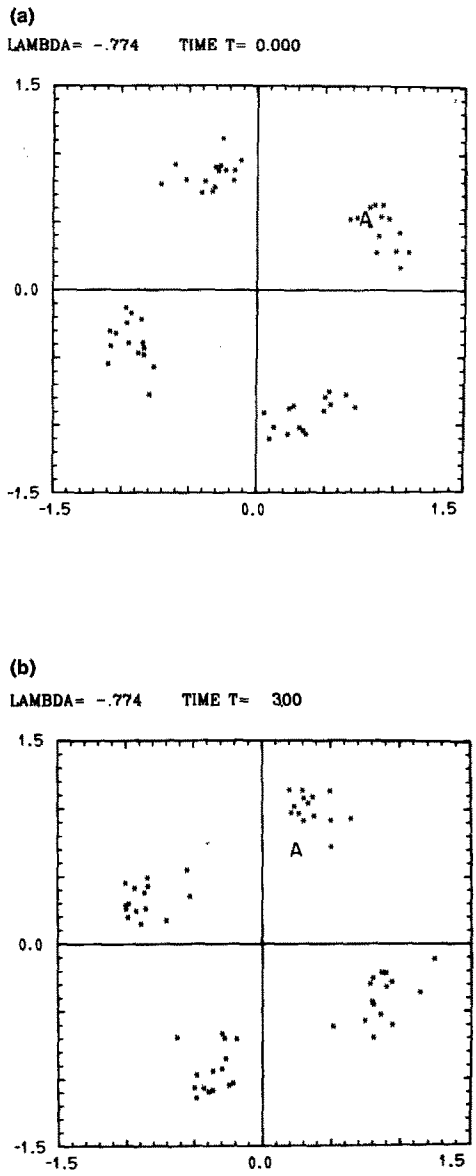

Fig. 7. Same as Fig. 6 with four-cluster initial configuration.

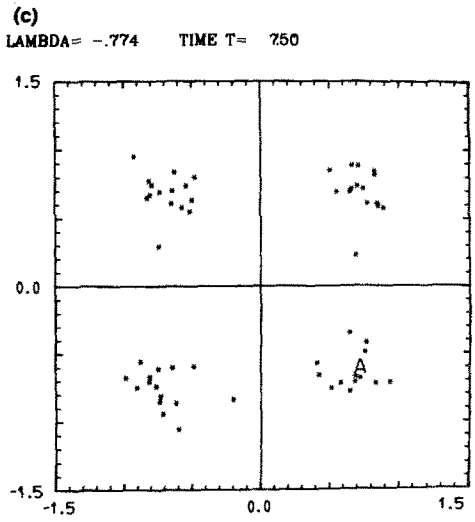

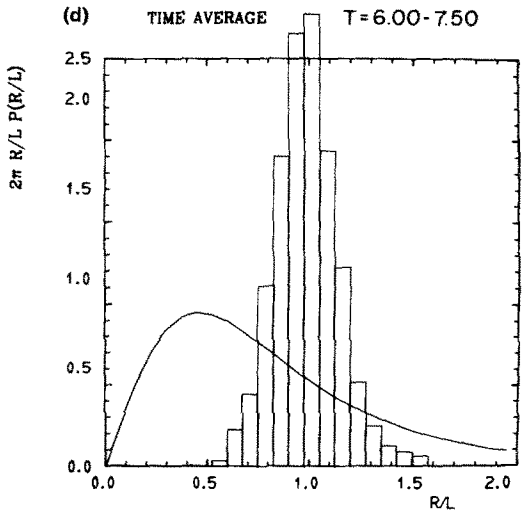

Fig. 7. Continued.

4.1. The Motion of a Cluster of Vortices in a Weak External Velocity Field

This problem will be sketched first. The application when the weak velocity field is produced by distant clusters will be discussed in a following subsection. The problem stated has general significance for two-dimensional turbulence since it describes the effect of "large eddies" on "small eddies." The method used below is a modification of Kubo's linear response theory.[38,39]

The equations of motion of N vortices in a given velocity field $\mathbf{V}(\mathbf{r}, t) = -\hat{\mathbf{z}} \times \nabla\psi(\mathbf{r}, t)$ are

$$\Gamma \frac{d\mathbf{r}_i}{dt} = -\hat{\mathbf{z}} \times \frac{\partial \mathscr{H}}{\partial \mathbf{r}_i} + \Gamma \mathbf{V}(\mathbf{r}_i, t) \tag{54}$$

The Liouville equation, with the external field, is

$$\frac{\partial P_N}{\partial t} + \frac{1}{\Gamma} \sum_{i=1}^{N} \left[-\hat{\mathbf{z}} \times \frac{\partial \mathscr{H}}{\partial \mathbf{r}_i} + \Gamma \mathbf{V}(\mathbf{r}_i, t) \right] \cdot \frac{\partial P_N}{\partial \mathbf{r}_i} = 0 \tag{55}$$

Define

$$\mathbf{R} = \left\langle \frac{1}{N} \sum_{i=1}^{N} \mathbf{r}_i \right\rangle \tag{56}$$

$$L^2 = \left\langle \frac{1}{N} \sum_{i=1}^{N} (\mathbf{r}_i - \mathbf{R})^2 \right\rangle \tag{57}$$

$$E = \langle \rho \mathscr{H} \rangle \tag{58}$$

These quantities are constants of the motion when $\mathbf{V} \equiv 0$. Equations for their rate of change may be derived by multiplying the Liouville equation by appropriate functions and integrating over all $\mathbf{r}_i$. The Liouville equation will be solved by assuming

$$P_N = P_N{}^0 + P_N{}' \tag{59}$$

where $P_N{}^0$ is the equilibrium solution evaluated at the *current* values of $\mathbf{R}$, L^2, and E, and $P_N{}'$ is a small perturbation from equilibrium, which will be taken linear in $\mathbf{V}$, neglecting quadratic and higher contributions. When P_N is decomposed as in Eq. (59) the equation for L^2 may be written

$$\frac{dL^2}{dt} = \frac{2}{N} \int \sum_{i=1}^{N} \eta_i \eta_i P_N{}' \, d\mathbf{r}_1 \cdots d\mathbf{r}_N : \frac{\partial \mathbf{V}(\mathbf{R}, t)}{\mathbf{R}} \tag{60}$$

with similar expressions for $\mathbf{R}$ and E. The quantity $\boldsymbol{\eta}_i$ is defined by $\boldsymbol{\eta}_i = \mathbf{r}_i - \mathbf{R}$. A Taylor expansion of the external field in powers of this quantity has been performed keeping the lowest order nontrivial terms. The assumption is that the external field is slowly varying over distances of order L, the size of the cluster. The expansion would be exact if the velocity field were a linear function of position.

Following Kubo, the equation for P_N' may be solved formally by integrating along the characteristics of the unperturbed Liouville operator. Omitting the details, this solution may be used to evaluate the integral in Eq. (60), thus establishing the result

$$\frac{dL^2}{dt} = \frac{8(1+\lambda)}{NL^2} \int_0^\infty R(\tau, t)\, d\tau\, D_{\alpha\beta} D_{\alpha\beta} \tag{61}$$

where

$$D_{\alpha\beta} = \frac{1}{2}\left(\frac{\partial V_\alpha}{\partial x_\beta} + \frac{\partial V_\beta}{\partial x_\alpha}\right)$$

is the rate of strain tensor of the external velocity field evaluated at the center of the cluster and

$$R(\tau, t) = \left\langle \left(\sum_{i=1}^{N} x_i y_i\right)_t \left(\sum_{i=1}^{N} x_i y_i\right)_{t+\tau} \right\rangle \tag{62}$$

is to be evaluated from the equilibrium ensemble using the values of the constants of integration at time t. In this expression x_i, y_i are the coordinates of a vortex relative to the center of vorticity.

The factor $\int_0^\infty R(\tau, t)\, d\tau$, being the integral of an autocorrelation function, is equal to the corresponding energy spectrum at zero frequency, which is known to be always nonnegative[40]; therefore L^2 never decreases with time, regardless of the external velocity field. The quantity $\frac{1}{4}\, dL^2/dt$ can be regarded as an eddy viscosity coefficient. As such, Eq. (61) says that the large eddies, represented by the external velocity field, have the effect of a positive viscosity on the small eddies, represented by the cluster of vortices. Note, also, that while *linear* response theory has been used, this result is quadratic in the weak velocity field.

Scaling all lengths with L and scaling the time with $T = (2\pi L)^2/N\Gamma$ as in Section 3, we can write the normalized autocorrelation

$$\begin{aligned} &S(\tilde{\tau}) = R(\tau)/R(0), \qquad \tilde{\tau} = \tau/T \\ &\int_0^\infty R(\tau)\, d\tau = R(0)T \int_0^\infty S(\tilde{\tau})\, d\tilde{\tau} \end{aligned} \tag{63}$$

where the zero-lag function $R(0)$ appears to scale like

$$R(0)/NL^4 = \sigma(\lambda) \tag{64}$$

In order to numerically evaluate the ensemble average the ergodic assumption[40] will be made, replacing the ensemble average by a time average in one member of the ensemble in the form

$$R(\tau) = (1/t_0)\int_0^{t_0} g(t)g(t+\tau)\,dt, \qquad g = \sum_{i=1}^{N}(x_i y_i) \tag{65}$$

The function g is evaluated by integrating Eq. (48) as described in Section 3 for a specified energy level with $N = 40$ and the computation is originally run for a long enough time that the system is near equilibrium. The lag function is computed with t_0 on the order of 60 time units, a very long time. However, since the accuracy of the computation as measured by reversibility is only about four time units, one cannot expect good results for lags much greater than this.

In Fig. 8, the normalized function $S(\tilde{\tau})$ is shown for $\lambda = 0.59$, compared with a damped cosine, which it resembles closely. The positive correlations occur about every turnaround time. Similar results could be shown for two other values of λ. Estimates of the value of $\int_0^\infty S(\tilde{\tau})\,d\tilde{\tau}$ have been obtained by integrating the damped cosine curve that best fits the first few cycles. These

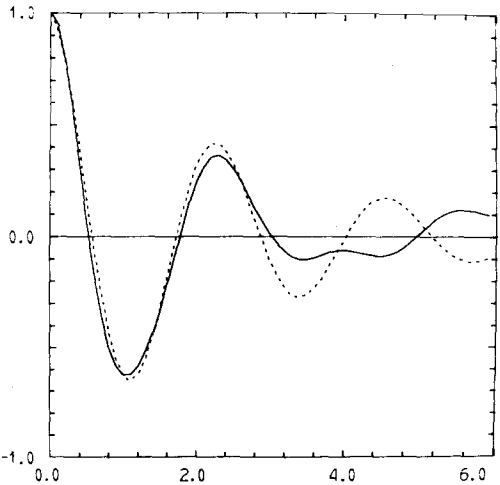

Fig. 8. Normalized autocorrelation of $\sum_{i=1}^{N}\chi_i y_i$ vs. the lag time in turnaround time units. Experimental points are computed from the equilibrium configuration with the energy level specified by $\lambda = 0.59$. Dotted line is an exponentially damped cosine, $\exp(-0.38t/T)\cos(2.7t/T)$.

Table I

λ	$\int_0^\infty S(\bar{\tau})\, d\bar{\tau}$	σ
14.5	0.023	0.25
0.59	0.05	0.24
−0.34	0.043	0.32

results are shown in Table I. While the results are not very accurate, they seem to support $\sigma \approx 0.25$, $\int_0^\infty S(\bar{\tau})\, d\bar{\tau} \approx 0.04$ for all λ.

4.2. Direct Simulation of Vortices in an External Field

A series of simulations of a cluster of vortices in an external field has been performed using Eq. (54) with an external field given by

$$\psi = a(\tfrac{3}{2}x^2 + \tfrac{1}{2}y^2) \tag{66}$$

a combined plane strain and solid body rotation. The 3/2, 1/2 combination is what one gets locally due to a distant "point" vortex cluster corotating with a cluster of the same strength, as seen in a coordinate frame in which the latter cluster is at rest. In this frame the "point" cluster is at some negative value of x.

A typical result is shown in Fig. 9 for 60 vortices, $\lambda_0 \approx 14$, with $aT_0 = 0.5$, a value too large for the linear response theory to hold. Figure 9a shows the initial configuration of the vortices, selected after a long run without the external field. Figure 9b is 0.83 time units later, when $L = 1.27L_0$. The noticeable skewing of the streamlines from a circular pattern to one stretched into the second and fourth quadrants is directly related to the growth of the cluster. This may be seen by calculation of L^2 from Eq. (54), with Eq. (66),

$$\frac{1}{2}\frac{dL^2}{dt} = -\frac{2a}{N}\sum_{i=1}^{N} x_i y_i \tag{67}$$

so that in order for L^2 to increase with time it is necessary that there be more vortices in the second and fourth quadrants than in the first and third.

In Fig. 10, the result of ensemble-averaging four runs with $aT_0 = 0.23$ and $\lambda_0 = 0.59$ is shown. The initial conditions were taken at intervals from the long run from which the autocorrelation in Fig. 8 was computed. The oscillations of L as it grows are related to the oscillations in this autocorrelation. Equation (61), which describes the rate of growth of L, involves a long-

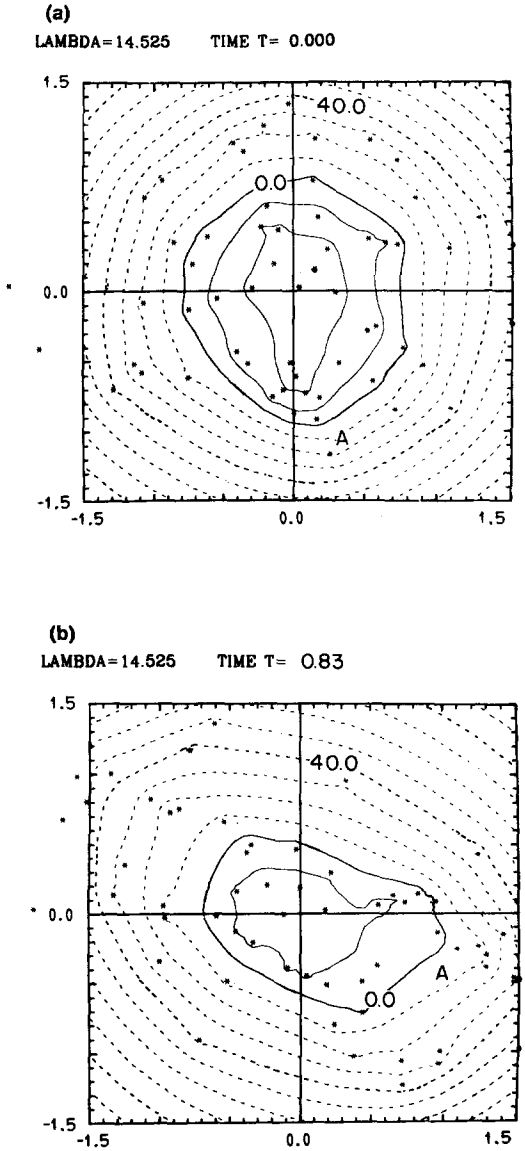

Fig. 9. Sixty vortices in an external velocity field similar to that produced by a point vortex off to the left of the figure. (a) Initial configuration shown by stars and streamlines, with energy level given by $\lambda = 14.5$. (b) Configuration 0.83 turnaround time units later, where $L = 1.127L_0$ and the vortex distribution is skewed into the second and fourth quadrants.

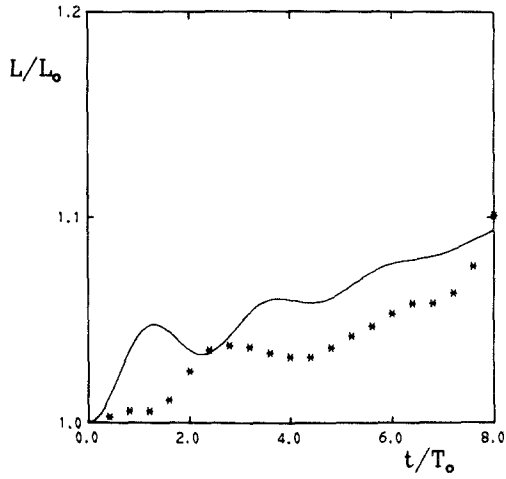

Fig. 10. Ensemble-average of four sets of 60 vortices in a weak external velocity field ($aT_0 = 0.23$), showing the cluster size L/L_0 vs. dimensionless time. The solid line is calculated from the linear response theory result using the damped cosine shown in Fig. 8 for the autocorrelation function.

time limit on the right side which integrates the autocorrelation to infinity. A form that is correct for short times also may be written

$$\frac{dL^2}{dt/T} = 16(1 + \lambda)\sigma L^2 \int_0^{t/T} S(\tilde{\tau})\, d\tilde{\tau} \left(\frac{1}{2} T^2 D_{ij} D_{ij}\right) \tag{68}$$

The solid line in Fig. 10 is the result of integrating Eq. (68) with S given by the damped cosine shown in Fig. 8. The agreement is not perfect, but has oscillations and the proper growth rate.

4.3. Argument for the Equilibration of Distant Clusters. Negative Viscosity

Consider a number of clusters of vortices, which in lowest approximation interact as point vortices. Equation (61) shows that each cluster will grow in size. In the definition of the constant of motion $NL^2 = \sum r_i^2$, the summation can be carried out over the vortices in each cluster, then over the clusters, giving

$$\sum_I N_I(R_I^2 + L_I^2) = \text{const} \tag{69}$$

where $\mathbf{R}_I$ is the center of the Ith cluster, and N_I is the number of vortices in the cluster. Since L_I^2 grows with time, it follows that $\sum N_I R_I^2$ decreases; therefore the clusters draw together, which shows the beginning of a tendency to equilibrate. The quantity

$$\frac{1}{4N} \sum_I N_I \frac{dR_I^2}{dt} \tag{70}$$

which can also be called an eddy viscosity, is negative.[41]

The decrease in $\sum N_I R_I^2$ corresponds to an increase in the angular momentum of the system of "point" clusters at the expense of the angular momentum of the internal structure of the clusters. This transport of momentum into the "zonal winds" is what is required in the earth's atmosphere to balance frictional losses[25] in the prevailing westerly winds. It is interesting that this atmospheric transport is associated with tilting of the troughs and ridges toward the east with increasing latitude and with a corresponding skewing of cyclones, similar to that seen in Fig. 9.

More specific results may be obtained for clusters of the same strength and size equally spaced around a circle by using Eq. (61) and the estimates from Table I. For two, three, or four clusters with N_1 in each cluster, each a distance R from the origin, $D_{ij}D_{ij} = (1/8, 2/9, 1/8)(N_1\Gamma/2\pi)^2(1/R^4)$, respectively. When this is used in Eqs. (63) and (61), the result

$$\frac{1}{R}\frac{dR}{dt/T} = -(0.10, 0.13, 0.05)(1 + \lambda)(L/R)^4$$

is obtained, where $T = (2\pi R)^2/N\Gamma$ is the approximate time for a cluster to orbit around the origin. The simulations of Figs. 5–7 are for two, three, or four clusters, respectively. In Fig. 5, the initial value of L/R is about unity, which, while too large for the formula to be applicable, nevertheless gives an equilibration time of several turnaround times. In Fig. 6, the initial value of L/R is about 0.5, which gives

$$\frac{1}{R}\frac{dR}{dt/T} \approx -10^{-2}$$

taking $\lambda = 0$, for lack of a better value. This means that the initial rate of decrease of R is such that R should decrease by about 3% in three turnaround times, a rate close to that observed. In Fig. 7, however, the initial value of L/R is only about 0.2 and the formula gives

$$\frac{1}{R}\frac{dR}{dt/T} \approx -10^{-4}$$

a rate only 1/100 of the previous case, or about 3% in 300 turnaround times.

This is too small to be observed during the time of the computation. The conclusion to be drawn is that the apparent failure to equilibrate in the simulation shown in Fig. 7 is consistent with the slow rate of equilibration predicted

Roberts and Christiansen[3] report clusters of vortices that fail to coalesce when the separation between the clusters is greater than a critical value. While the theory developed above, which appears to be in conflict with this, does not strictly apply, since Roberts and Christiansen's vortices are in a box, not in infinite space, and consequently $\sum r_i^2$ is not a constant of motion, it is possible, nevertheless, that the clusters would ultimately coalesce. There is a more important point to consider: Their "clusters of vortices" are really regions of uniform vorticity, which are described numerically by uniform distributions of vortices. Because of incompressibility, such regions of uniform vorticity cannot grow in size, though the simulating system of vortices can. This suggests that some caution should be exercised in interpreting numerical experiments where continuous distributions of vorticity have been replaced by discrete ones.

5. CONCLUSION

It is concluded that a cluster of vortices in an infinite space will tend to arrange itself in the axially symmetric configuration predicted from the microcanonical ensemble. The structure of the configuration depends on a parameter that was identified as the temperature. The fact that this temperature can be negative when the energy is greater than a critical value plays no essential role in the analysis and it could be considered to be merely a function of energy defined by Eq. (9).

There is no thermodynamic scaling in the problem treated here. The energy scales with N^2, the temperature scales with N.

A difficulty in the numerical experiments was the apparent failure of distant clusters to coalesce into a single equilibrium cluster. It was shown in Section 4, by using linear response theory, that a very slow rate of equilibration is to be expected in this case. This result, expressed by Eq. (61), is the most important result in this paper. It shows that a cluster of vortices in a weak external velocity field will grow in size due to the influence of the external field, a nonequilibrium result. The significance is that the large eddies in a two-dimensional vortex flow have the effect of a positive eddy viscosity on the small eddies. A consequence of this result is that in a system made up of a large number of weakly interacting clusters the individual clusters will grow in size while the centers of vorticity of the clusters tend to collapse together. The latter effect is in the nature of a global negative eddy viscosity.

ACKNOWLEDGMENTS

The authors would like to acknowledge useful discussions with J. R. Herring, G. R. North, and P. D. Thompson.

REFERENCES

1. F. H. Abernathy and R. E. Kronauer, *J. Fluid Mech.* **13**:1 (1961).
2. G. S. Beavers and T. Wilson, *J. Fluid Mech.* **44**:97 (1970).
3. K. V. Roberts and J. P. Christiansen, *Computer Phys. Comm.* **3**, Suppl. 14 (1972).
4. J. P. Christiansen, *J. Comp. Phys.* **13**:363 (1973).
5. J. P. Christiansen and N. J. Zabusky, *J. Fluid Mech.* **61**:219 (1973).
6. A. L. Fetter, *Phys. Rev.* **152**:183 (1966).
7. A. L. Fetter, *Phys. Rev.* **153**:285 (1967).
8. G. B. Hess, *Phys. Rev.* **161**:189 (1967).
9. D. Stauffer and A. L. Fetter, *Phys. Rev.* **168**:156 (1968).
10. C. H. Su, *Phys. Fluids* **16**:182 (1973).
11. G. A. Williams and R. E. Packard, *Phys. Rev. Lett.* **33**:280 (1974).
12. L. Onsager, *Nuovo Cimento Suppl.* **6**:229 (1949).
13. J. B. Taylor and B. McNamara, *Phys. Fluids* **14**:1492 (1971).
14. G. Vahala and D. Montgomery, *Plasma Phys.* **6**:425 (1971).
15. D. Montgomery, *Phys. Lett.* **A39**:7 (1972).
16. J. B. Taylor, *Phys. Lett.* **A40**:1 (1972).
17. J. P. Christiansen and J. B. Taylor, *Plasma Phys.* **15**:585 (1973).
18. G. Joyce and D. Montgomery, *J. Plasma Phys.* **10**:107 (1973).
19. S. F. Edwards and J. B. Taylor, *Proc. Roy. Soc. Lond. A* **336**:257 (1974).
20. C. E. Seyler, Jr., *Phys. Rev. Lett.* **32**:515 (1974).
21. D. Montgomery and G. Joyce, *Phys. Fluids* **17**:1139 (1974).
22. D. Montgomery, in *Plasma Physics: Les Houches 1972* (Gordon and Breach, 1975).
23. S. Putterman, *Phys. Reports* (*Sect. C of Phys. Lett.*) **4**(2):67 (1972).
24. E. Palmen and C. W. Newton, *Atmospheric Circulation Systems* (Academic Press, New York, 1969), p. 328.
25. E. N. Lorenz, *The Nature and Theory of the General Circulation of the Atmosphere* (World Met. Org., 1967), p. 78.
26. H. Lamb, *Hydrodynamics* (Dover, New York, 1945), p. 230.
27. G. E. Uhlenbeck and G. W. Ford, *Lectures in Statistical Mechanics* (American Math. Soc., Providence, R.I., 1963), p. 3.
28. A. Khinchine, *Mathematical Foundations of Statistical Mechanics* (Dover, New York, 1949).
29. J. L. Lebowitz and O. Penrose, *Phys. Today* **1973** (Feburyary 23).
30. L. Landau and E. Lifshitz, *Statistical Mechanics* (Pergamon Press, 1958), p. 25.
31. K. Huang, *Statistical Mechanics* (Wiley, New York, 1963), Chapter 7.
32. A. M. Salzberg and S. Prager, *J. Chem. Phys.* **38**:2587 (1963).
33. D. C. Montgomery and D. A. Tidman, *Plasma Kinetic Theory* (McGraw-Hill, New York, 1964), p. 46.
34. A. Nordsieck, *Math. Comp.* **16**:22 (1962).
35. J. J. Thomson, *A Treatise on the Motion of Vortex Rings* (McMillan and Co., London, 1883).
36. T. H. Havelock, *Phil. Mag. S7* **11** (No. 70, Supp. Feb.) (1931).

37. G. K. Morikawa and E. V. Swenson, *Phys. Fluids* **14**:1058 (1971).
38. R. Kubo, *J. Phys. Soc. Japan* **12**:570 (1957).
39. R. Kubo, in *Many-Body Problems*, Parry *et al.*, eds. (Benjamin, New York, 1969).
40. A. Papoulis, *Probability, Random Variables and Stochastic Processes* (McGraw-Hill, New York, 1968).
41. V. P. Starr, *Physics of Negative Viscosity Phenomena* (McGraw-Hill, New York, 1968).